Chapter 2: Rigid Bar Supported by Two Buckled Struts under Axial, Harmonic, Displacement Excitation

2.1 Introduction

The model studied in this chapter is a simple system of two buckled struts supporting a bar that is assumed to be rigid. As mentioned previously, the main difference between the work in this research and the previous work performed on buckled struts as vibration isolators by Alloway (2003), Plaut et al. (2003), and Sidbury (2003) is that the system is comprised of two struts connected by a rigid bar, instead of one strut supporting a mass. The previous work determined that the behavior of the buckled strut under axial, harmonic, displacement excitation was similar for fixed-end conditions versus pinned end conditions of the struts (Sidbury, 2003). Therefore, fixed-end boundary conditions were chosen for this research because they can support more load and are easier to model physically.

The first step is to develop and analyze the simple system of a symmetric bar supported by two buckled struts. The system is analyzed first to obtain the equilibrium state, and these results are used to analyze the system under forced vertical harmonic excitation at the base. Because the system is symmetric and there is no rotation of the bar, the analytical procedure and results are the same as for the fixed-end buckled single-strut case of the previous work mentioned above. Next, the rigid bar is assumed to be asymmetric, which loads each strut differently and creates a rotation of the bar. Again, the system is first evaluated for the equilibrium state, and the results are used to analyze the response under forced harmonic excitation at the base. Finally, with the bar remaining asymmetric, the stiffnesses of the vertical struts are varied so there is no rotation of the bar in equilibrium, and the system is analyzed in the same way as the first two models.

2.2 General Model Description

All the equations presented in this paper were developed by Dr. Raymond H. Plaut. Figure 2.1 shows the general model to be analyzed, in an undeformed state.

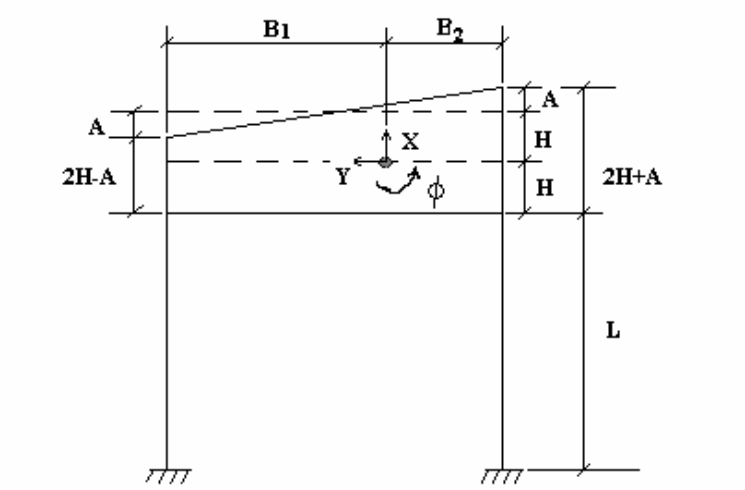

Figure 2.1 Rigid Bar Supported by Fixed-End Struts – Undeformed Shape

The variables used to describe the model are as follows:

L = the length of each strut, assumed to be equal

H = the distance from the bottom of the rigid bar to its centroid when A = 0

A = the distance from the reference line 2H above the bottom of the rigid bar to the top of the rigid bar at either end.

B_1 = the distance from the left end of the rigid bar to its centroid

B_2 = the distance from the right end of the rigid bar to its centroid

Φ = the angle of rotation of the rigid bar, measured from the horizontal

When A is equal to zero, the height of the rigid bar is 2H, B_1 is equal to B_2, and the angle of rotation Φ is equal to zero. This will be considered a symmetric rigid bar, and is the first case to be analyzed.

2. 3 Symmetric Bar

2.3.1 Equilibrium Analysis Procedure

The first step of the analysis is to evaluate the model at static equilibrium in a post buckled state. The model in a post-buckled static equilibrium state is shown in Figure

2.2. It should be noted that the model is constrained against any lateral movement. If it is free to move laterally, the model is unstable and would buckle under sway.

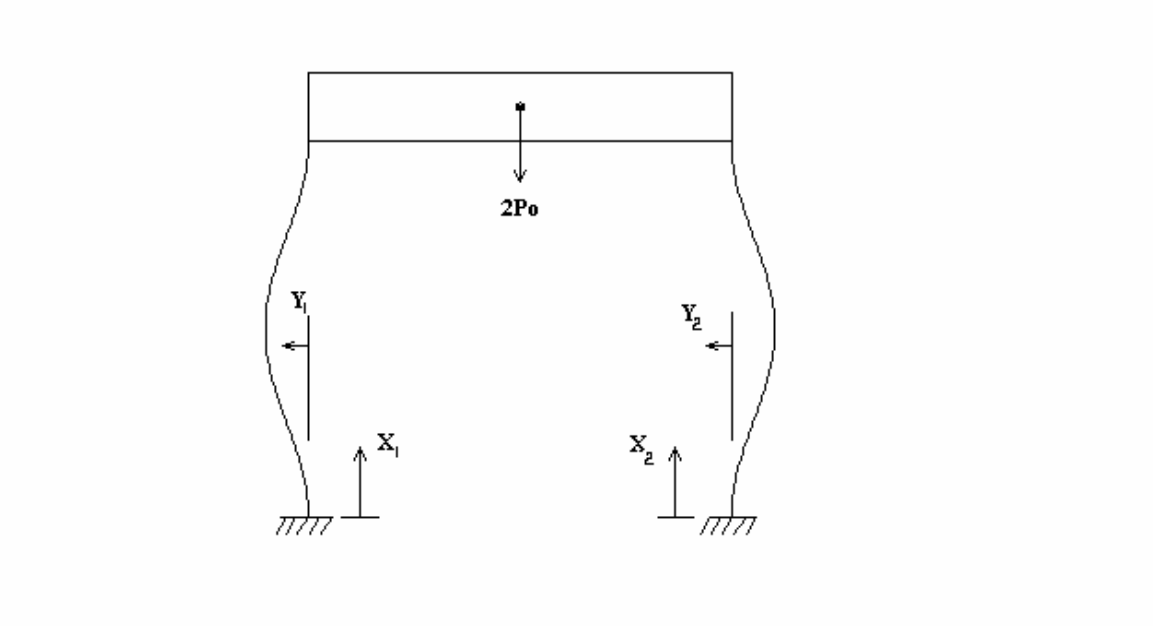

Figure 2.2 Post-Buckled Strut Equilibrium – Symmetric Bar

Because the bar is symmetric and the struts are assumed to have the same length and bending stiffness, analysis is done on one strut, and the other strut is assumed to be its mirror image. Figure 2.3 shows a single buckled strut in a horizontal position.

Figure 2.3 Single Buckled Strut Under Static Load P_o

The post-buckled state is achieved by loading the strut just above its Euler buckling load. (Hence, the full model will be loaded at twice this value, because there are two struts.) The strut is assumed to be an elastica, which means there is no axial deformation of the strut along its length. When the strut is evaluated in the equilibrium state, it is permitted

to have large deflections in the X and Y directions. Therefore, the angle θ can be used to measure the curvature of the strut, and it is considered to be a function of the arc length.

The variables shown in Figure 2.3 are as follows:

L = the length of the strut
S = the arc length of the strut
P_o = the applied load from the rigid bar on the strut
θ = the angle of the deflected strut measured from the X axis

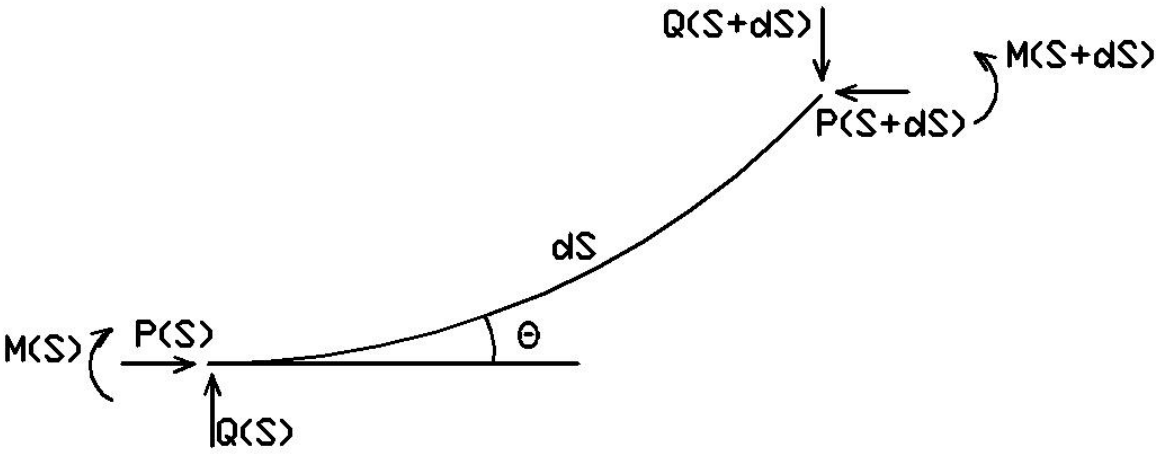

Figure 2.4 Free Body Diagram of Element of Strut in Equilibrium

A free body diagram of a small element of the strut is shown in Figure 2.4, and the additional variables associated with the free body diagram needed to evaluate the strut in static equilibrium are:

P = the horizontal component of force in the strut (as shown in the horizontal position)
Q = the vertical component of force in the strut (as shown in the horizontal position)
E = the modulus of elasticity of the strut
I = the moment of inertia of the cross section of the strut about the axis of bending
dS = small element of length along the arc of the strut
dX = projection of dS in the X direction
dY = projection of dS in the Y direction

Using the variables described above, the following equations can be written to describe the shape of the strut:

$$\frac{dX}{dS} = \cos\theta \tag{2.1}$$

$$\frac{dY}{dS} = \sin\theta \tag{2.2}$$

$$\frac{d\theta}{dS} = Curvature \tag{2.3}$$

$$M = EI\frac{d\theta}{dS} \tag{2.4}$$

$$\frac{dM}{dS} = -P\sin\theta + Q\cos\theta \tag{2.5}$$

All of the analysis is performed in nondimensional terms. The variables have been nondimensionalized so that the analysis provides valid results for any elastic material regardless of its value of modulus of elasticity E, and for any cross-sectional shape regardless of its value of moment of inertia I. In this way, results are not limited to specific materials or cross-sectional shapes. The variables have been nondimensionalized as follows:

$$x = \frac{X}{L} \qquad y = \frac{Y}{L} \qquad s = \frac{S}{L} \tag{2.6, 2.7, 2.8}$$

$$q = \frac{QL^2}{EI} \qquad p = \frac{PL^2}{EI} \qquad m = \frac{ML}{EI} \tag{2.9, 2.10, 2.11}$$

To obtain a post-buckled state of interest, the strut should be loaded slightly above the buckling load. For a strut with fixed-end conditions at both ends, this critical load is $P_o = 4\pi^2 EI/L^2$. The nondimensional buckling load, $p_{cr} = P_o L^2/EI$ has the value $p_{cr} = 4\pi^2 \approx 39.478$. A static value of $p_o = 40$ will be used in the analysis. (Hence, an initial nondimensional load of $p_o = 80$ will be applied to the entire system because there are two struts.) When the nondimensional variables shown in Equations 2.6 through 2.11 are

used in Equations 2.1, 2.2, 2.4, and 2.5, the result is the following differential equations for $0 < s < 1$:

$$\frac{dx}{ds} = \cos\theta \tag{2.12}$$

$$\frac{dy}{ds} = \sin\theta \tag{2.13}$$

$$\frac{d\theta}{ds} = m \tag{2.14}$$

$$\frac{dm}{ds} = -p\sin\theta + q\cos\theta \tag{2.15}$$

Boundary conditions must be established to complement the differential equations. The fixed-end condition of the strut does not allow any rotation at the ends of the strut, nor does it allow any deflection in the y direction (as shown in the horizontal position). Therefore, the boundary conditions used to solve the system of differential equations for the fixed-end condition are as follows:

At s = 0: x = 0, y = 0, and θ = 0 (the left, or bottom, end of the strut)
At s = 1: y = 0, and θ = 0 (the right, or top, end of the strut)

A Mathematica program was written to solve the system of equations. Based on a given value for the initial load p_o, the program solves for the values of the moment m and the shear force q at the left end, or bottom, of the strut (at s = 0). The program utilizes a shooting method, which is an iterative process in which initial guesses are given for m and q, and the solution is found by an iterative procedure. A text printout of the program is provided in Appendix A.

2.3.2 Dynamic Analysis Procedure

The model is subjected to a forced harmonic vibration (axial base displacement), as discussed in Chapter 1, given by Equation 1.1. Again, showing the strut in the horizontal

position in Figure 2.5, the base is at the left, and the excitation is shown acting on the base. The reaction force at the top (or right end) is given as the mass of the system (weight W divided by the gravitational acceleration g) multiplied by the acceleration of the system, which is the second derivative of the position function (refer to Equation 1.5) plus the static force W. Note that now the deflection is a function of position along the strut *and* time.

Figure 2.5 Strut Under Forced Harmonic Vibration

The variables used in the dynamic analysis are listed below:

T = time
W = weight of supported load (half of rigid bar)
Ω = applied frequency
$U_o \sin(\Omega T)$ = axial displacement of base of strut (in X direction)
g = acceleration of gravity
μ = mass per unit length of the strut
P_w = the ratio of the weight W to the weight μgl of the strut
r = stiffness parameter
C = external damping coefficient

The new variables introduced above are also nondimensionalized in the same way as the first set of variables in Equations 2.6 – 2.11. These equations are shown below:

Time: $t = T\sqrt{\dfrac{EI}{\mu L^4}}$ (2.16)

Frequency: $\omega = \Omega\sqrt{\frac{\mu L^4}{EI}}$ (2.17)

Base Displacement Amplitude: $u_o = \frac{U_o}{L}$ (2.18)

Forces: $p_w = \frac{W}{\mu g L}, \quad p_o = \frac{WL^2}{EI}$ (2.19, 2.20)

Stiffness Parameter: $r = \frac{p_w}{p_o} = \frac{EI}{\mu g L^3}$ (2.21)

External Damping Parameter: $c = \frac{CL^2}{\sqrt{\mu EI}}$ (2.22)

Damping is assumed to be viscous damping, i.e., the relationship between the damping force and the velocity of the system is linear. Damping will not be varied much within the experiments to be performed. This is due to the fact that damping is difficult to model. It can not be determined from the size, dimensions, material, or other physical properties of an element. It must be determined through experiments such as a free-vibration test. But it is present and must be accounted for in the analysis.

To analyze the strut under forced harmonic excitation, a free body diagram of forces acting on an element at a particular time and position can be drawn. This is done using D'Alembert's Principle, which uses a fictitious *inertia force* that is equal to the product of the mass and the acceleration. This force is assumed to act in the opposite direction of the accelerating mass, therefore at a particular instant in time, the strut is considered to be in a state of static equilibrium (Chopra, 2001). The damping force is also included in the free body diagram - see Figure 2.6.

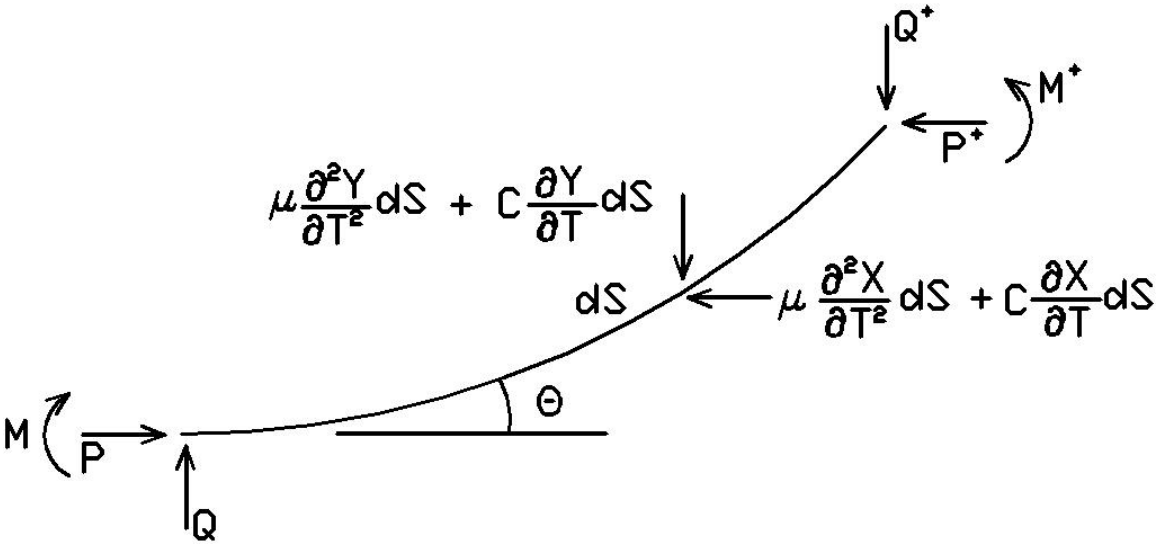

Figure 2.6 Free Body Diagram of Element of Strut Under Forced Harmonic Vibrations

Using this free body diagram, the following relationships can be written (prior to nondimensionalizing the terms):

$$\frac{\partial X}{\partial S} = cos\,\theta \tag{2.23}$$

$$\frac{\partial Y}{\partial S} = \sin\theta \tag{2.24}$$

$$\frac{\partial \theta}{\partial S} = \frac{M}{EI} \tag{2.25}$$

$$\frac{\partial M}{\partial S} = -P\sin\theta + Q\cos\theta \tag{2.26}$$

$$\frac{\partial P}{\partial S} = -\mu\frac{\partial^2 X}{\partial T^2} - C\frac{\partial X}{\partial T} \tag{2.27}$$

$$\frac{\partial Q}{\partial S} = -\mu\frac{\partial^2 Y}{\partial T^2} - C\frac{\partial Y}{\partial T} \tag{2.28}$$

The following differential equations can now be written using the equilibrium relationships, for values of s between 0 and 1:

$$\frac{\partial x}{\partial s} = \cos\theta \tag{2.29}$$

$$\frac{\partial y}{\partial s} = \sin\theta \tag{2.30}$$

$$\frac{\partial \theta}{\partial s} = m \tag{2.31}$$

$$\frac{\partial m}{\partial s} = \frac{\partial \theta}{\partial s} \tag{2.32}$$

$$\frac{\partial p}{\partial s} = -\frac{\partial^2 x}{\partial t^2} - c\frac{\partial x}{\partial t} \tag{2.33}$$

$$\frac{\partial q}{\partial s} = -\frac{\partial^2 y}{\partial t^2} - c\frac{\partial y}{\partial t} \tag{2.34}$$

Each variable that describes the strut can now be written as a function of time and location along the strut to describe the response of the strut to the forced excitation. The subscript "e" represents the equilibrium portion of the equation, and "d" represents the dynamic portion. These equations, in nondimensional terms, are written below:

$$x(s,t) = x_e(s) + x_d(s)e^{i\omega t} \tag{2.35}$$

$$y(s,t) = y_e(s) + y_d(s)e^{i\omega t} \tag{2.36}$$

$$\theta(s,t) = \theta_e(s) + \theta_d(s)e^{i\omega t} \tag{2.37}$$

$$m(s,t) = m_e(s) + m_d(s)e^{i\omega t} \tag{2.38}$$

$$p(s,t) = p_o + p_d(s)e^{i\omega t} \tag{2.39}$$

$$q(s,t) = q_e + q_d(s)e^{i\omega t} \tag{2.40}$$

It is assumed that the dynamic vibrations will be very small, and small displacement theory can be used to determine the following linear dynamic relationships:

$$\frac{dx_d}{ds} = -\theta_d \sin\theta_e \tag{2.41}$$

$$\frac{dy_d}{ds} = \theta_d \cos\theta_e \tag{2.42}$$

$$\frac{d\theta_d}{ds} = m_d \tag{2.43}$$

$$\frac{dm_d}{ds} = (q_d - p_o\theta_d)\cos\theta_e - (p_d + q_e\theta_d)\sin\theta_e \tag{2.44}$$

$$\frac{dp_d}{ds} = (\omega^2 - i\omega c)x_d \tag{2.45}$$

$$\frac{dq_d}{ds} = (\omega^2 - i\omega c)y_d \tag{2.46}$$

The final equations required to solve the system of differential equations are the boundary conditions at each end of the strut. In nondimensional terms, they are:

At s=0: $x_d = u_o,\ y_d = 0,\ \theta_d = 0$ (the left, or bottom end of the strut)
At s=1: $y_d = 0,\ \theta_d = 0$ (the right, or top end of the strut)

A program was written in Mathematica to solve the system of differential equations, similar to the program used to solve the static equilibrium equations. The values for the moment m_e and shear force q_e determined from the equilibrium analysis are used as input in the dynamic analysis to determine the transmissibility. Also, known values of the initial load p_o, the amplitude of the excitation at the base u_o, the stiffness parameter r, and the external damping parameter c are used as input in the program. It then utilizes a "do" loop to solve for the transmissibility of the system for a range of nondimensional frequency values, ω. As before, it uses a shooting method to solve the equations. Initial guesses are given for the values of $p_d(0)$, $q_d(0)$, and $m_d(0)$. To aid in the speed of the program, the results for the values of $p_d(0)$, $q_d(0)$, and $m_d(0)$, or some percentage of their

values, are then used as the guess for the next run in the loop. Appendix B shows a text printout of this program.

The transmissibility of the system is the ultimate goal of this calculation, and indeed this research as a whole. The equation used to determine the transmissibility is shown below

$$TR = \frac{\sqrt{\{Re[x_d(1)]\}^2 + \{I_m[x_d(1)]\}^2}}{|u_o|} \tag{2.47}$$

As mentioned before, this is a displacement transmissibility. The equation utilizes the capabilities of the computer program to solve for the real and imaginary parts of the solution. The resulting value used for the position of the strut at the top due to the dynamic load is the square root of the sum of the squares (SRSS) of the real and imaginary values. This, of course, is divided by the original amplitude of the base, u_o, to determine the transmissibility. Because each strut is forced at the same amplitude and frequency, the transmissibility calculated for the top of each strut is also the transmissibility at the center of the rigid bar.

Another useful characteristic of the system to determine are its resonant frequencies. A resonant frequency can be determined by locating a frequency at which an undamped system's transmissibility is infinite. By setting the value of the external damping parameter c equal to zero, the undamped case can be analyzed and the resonant frequencies can be found. When transmissibility is plotted versus the nondimensional frequency ω, the resonant frequencies are easily located in the undamped case by the high peaks on the plot. Also, as long as the system's damping is below the critical damping value, the transmissibility plots for damped cases will still show peaks near these resonant frequency locations. (A system is considered critically damped or overdamped when it does not oscillate under a free vibration situation.) As the value of c increases and approaches its critical value, the transmissibility at a resonant frequency tends to decrease.

2.3.3 Results for Symmetric Bar

The transmissibility of the system was calculated for a range of nondimensional applied frequencies from 0.1 to 200. For the case c = 1, r = 1, and p_o = 40, it is plotted against the frequency in Figure 2.7. As can be seen, four peaks in the transmissibility values are noted. These peak frequencies are located at ω = 0.69, 44.7, 75.3, and 173.7. It was mentioned previously that a vibration isolator is only useful when the transmissibility is below unity. As can be seen in the plot, there is a wide range of frequencies for which this is the case. For values of ω between approximately 1 and 70, the transmissibility is well below a value of 1. The transmissibilities of the peak frequencies other than the first peak are equal to or below 1 as well.

It is also interesting to observe the vibration of the model at each of these peak frequencies. This is also shown in Figure 2.7. The dark line in each of the vibration shapes shows the model in equilibrium, before it is subjected to the harmonic excitation. The two lighter lines show the shape of the vibrating struts at each peak frequency. The vibration shape at the first peak, ω = 0.69, shows greater movement of the rigid bar above and below the equilibrium state compared to the other three shapes. This is expected because the transmissibility at this peak is much higher. The vibration shape of the struts at ω = 0.69 is similar to the equilibrium shape, i.e., there are no nodes. The vibration shapes of the struts at the second and fourth peak frequencies show very noticeable nodes. One node is present at the second peak, and three nodes can be seen at the fourth peak. It is interesting to note that there are no nodes at the third peak.

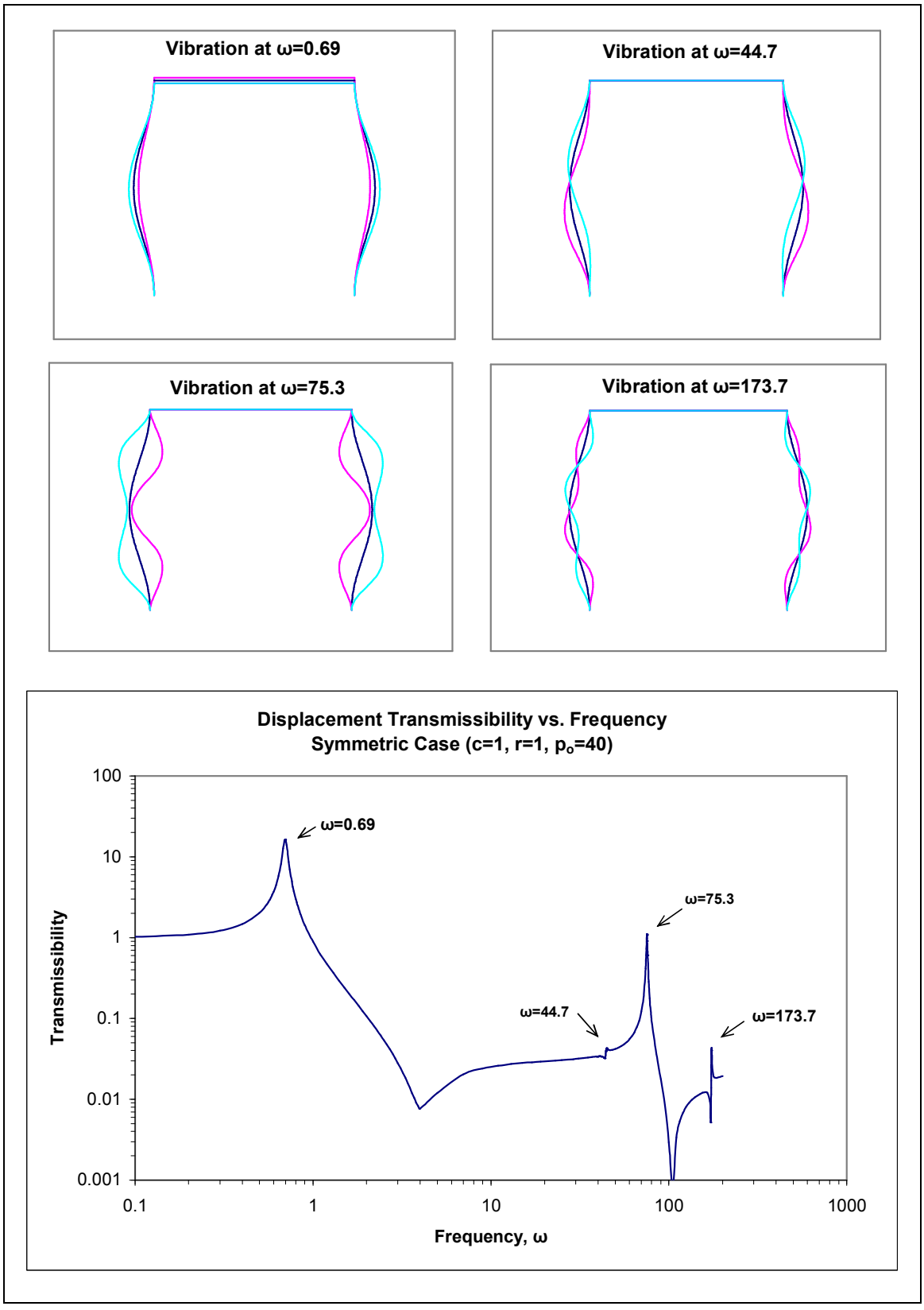

Figure 2.7 Transmissibility vs. Frequency with Vibration Shapes

2.4 Asymmetric Bar

The case of the perfectly symmetric rigid bar is of course ideal, but is useful for studying the effectiveness of post-buckled struts as vibration isolators. Results from Sidbury (2003) are applicable for the symmetric case. Because physical objects are rarely perfectly symmetrical, it was decided to study the performance of the buckled struts supporting an asymmetric load. Referring to Figure 2.1, a value of A is given other than zero so that the bar is asymmetrical. Now B_1 does not equal B_2, and if A is positive, the centroid of the bar shifts to the right of center. Also, there is now rotation of the bar. A constant density of the bar is assumed, so that the center of mass is at the same location as the geometric centroid. Therefore, each strut is supporting a different static load. The system can no longer be analyzed by evaluating one strut because the struts are no longer mirror images of each other. As before, the system must be analyzed in an equilibrium state first, and then the solutions from the equilibrium analysis are used in the dynamic analysis.

2.4.1 Equilibrium Analysis Procedure

Figure 2.8 below shows the system in its deformed shape under the applied static load. As before, it is constrained against lateral movement for stability.

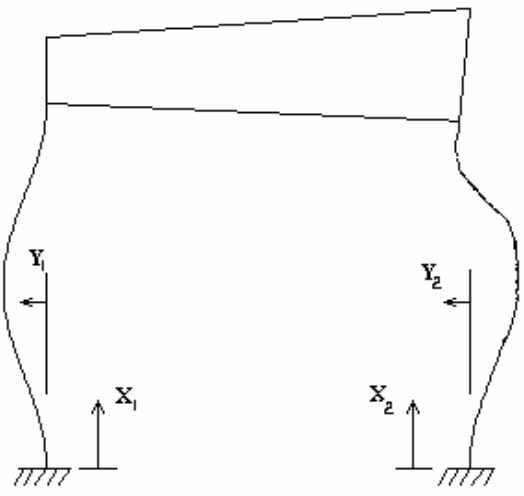

Figure 2.8 Post-Buckled Equilibrium State – Asymmetric Case

The same nondimensional quantities used in the single-strut analysis will be used here, except each strut will have its own set of variables, designated by a subscript 1 for the left strut and 2 for the right strut:

$$x_1 = \frac{X_1}{L};\ x_2 = \frac{X_2}{L} \qquad y_1 = \frac{Y_1}{L};\ y_2 = \frac{Y_2}{L} \qquad (2.48, 2.49, 2.50, 2.51)$$

$$s_1 = \frac{S_1}{L};\ s_2 = \frac{S_2}{L} \qquad q_1 = \frac{Q_1 L^2}{EI};\ q_2 = \frac{Q_2 L^2}{EI} \qquad (2.52, 2.53, 2.54, 2.55)$$

$$p_1 = \frac{P_1 L^2}{EI};\ p_2 = \frac{P_2 L^2}{EI} \qquad m_1 = \frac{M_1 L}{EI};\quad m_2 = \frac{M_2 L}{EI} \qquad (2.56, 2.57, 2.58, 2.59)$$

In addition, the following variables are nondimensionalized:

$$a = \frac{A}{L} \qquad h = \frac{H}{L} \qquad b_1 = \frac{B_1}{L} \qquad (2.60, 2.61, 2.62)$$

$$b_2 = \frac{B_2}{L} \qquad p_o = \frac{WL^2}{2EI} \qquad (2.63, 2.64)$$

A free body diagram of the rigid bar is drawn in Figure 2.9 to show the forces acting in static equilibrium. The forces from the struts are at s = 1 (top of the strut). In the symmetric case, m_1 and m_2 were equal and opposite values, and p_1 equaled p_2 which equaled p_o. When the bar is asymmetric, this is not the case. Separate values must be determined for each strut.

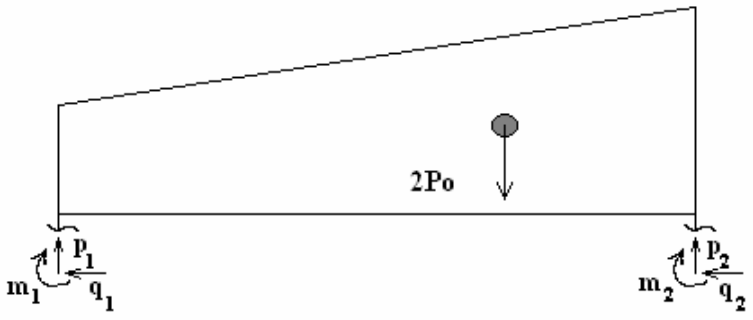

Figure 2.9 Free Body Diagram of Static Forces on Rigid Bar

From the free body diagram shown above, the following equations are written:

$$p_1 + p_2 = 2p_o \tag{2.64}$$

$$q_1 + q_2 = 0 \tag{2.65}$$

$$(p_2 b_2 - p_1 b_1)[b_1 + b_2 + y_1(1) - y_2(1)] + (q_2 b_2 - q_1 b_1 + 2p_o h)[x_2(1) - x_1(1)] = (b_1 + b_2)[m_1(1) + m_2(1)] \tag{2.66}$$

$$\sin\phi = \frac{x_2(1) - x_1(1)}{b_1 + b_2} \tag{2.67}$$

$$\cos\phi = \frac{y_1(1) - y_2(1)}{b_1 + b_2} + 1 \tag{2.68}$$

Also, the same equations written from the free body diagram of the single strut will apply to the struts (Equations 2.12 – 2.15). But again, each strut will have its own set of equations, using the same subscript notation:

$$\frac{dx_1}{ds_1} = \cos\theta_1 \qquad \frac{dx_2}{ds_2} = \cos\theta_2 \tag{2.69, 2.70}$$

$$\frac{dy_1}{ds_1} = \sin\theta_1 \qquad \frac{dy_2}{ds_2} = \sin\theta_2 \tag{2.71, 2.72}$$

$$\frac{d\theta_1}{ds_1} = m_1 \qquad \frac{d\theta_2}{ds_2} = m_2 \tag{2.73, 2.74}$$

$$\frac{dm_1}{ds_1} = -p_1\sin\theta_1 + q_1\cos\theta_1 \qquad \frac{dm_2}{ds_2} = -p_2\sin\theta_2 + q_2\cos\theta_2 \tag{2.75, 2.76}$$

The final set of equations needed to solve the differential equations are the boundary conditions at the ends of each strut. Assuming fixed-end conditions, they are as follows:

At $s_{1,2} = 0$: $\quad x_{1,2} = 0, \quad y_{1,2} = 0, \quad \theta_{1,2} = 0$

At $s_{1,2} = 1$: $\quad \sin\theta_{1,2} = \dfrac{x_2(1) - x_1(1)}{b_1 + b_2} \qquad \cos\theta_{1,2} = \dfrac{y_1(1) - y_2(1)}{b_1 + b_2} + 1$

For the boundary condition equation used at the top of the strut (s = 1), it has been assumed that the angle of rotation Φ of the rigid bar is the same as the angle θ of the strut. This assumption can be made because the struts are assumed to be fixed to the rigid bar, which allows no rotation with reference to the strut itself. If the rigid bar rotates, the struts will rotate by the same amount.

A Mathematica program was again written to solve the system's differential equations. As in the case of one strut, the value of the static load p_o is known. In addition, values are assigned to "a", b and h for the rigid bar. The value b = 0.5 is used so that the length of the bar is equal to the length of each strut. This value is used for all analyses of the asymmetric bar. By varying the value of "a", different asymmetric cases can be studied. A text printout of the Mathematica program can be found in Appendix C.

2.4.2 Equilibrium Results

For verification of the equilibrium program written for the asymmetric case, it was first evaluated for the symmetric case a = 0. This results in $b_1 = b_2$, hence the bar is symmetric. The equilibrium results for the values of the moment and shear force in the struts were equal for each strut, and their value ($m = 2.04$ and $q \cong 0$) was equal to the moment and shear force values determined for the symmetric case analysis using a single strut. Therefore, the program was verified for this special case.

It should also be mentioned that the direction of the buckled struts for the symmetric case can be outward as shown, or inward (the struts would be buckled towards each other

rather than away from each other). By giving the program initial guesses of a positive value for m_1 (the left strut) and a negative value for m_2 (the right strut), the struts are buckled away from each other (outward). By reversing the sign of the initial guesses, the struts are buckled inward. The inward buckled case was analyzed on the model and it did not change the magnitude of the equilibrium moment or shear force in the struts. However, when the asymmetric cases were analyzed ($a \neq 0$), the program did not give reasonable values for moments and shears in the struts unless they were buckled outward. Therefore, the outward buckled case is the appropriate condition for asymmetric equilibrium and was used for the remainder of the equilibrium and dynamic analysis.

Table 2.1 shows the values of "a" that were used for the dynamic analysis, which will be discussed later, and the corresponding values of b_1. When $a = 0$, then $b_1 = 0.5$, and the bar is symmetric.

Table 2.1 Values of "a" and the Corresponding b_1 Value

a	0	0.008	0.02	0.04	0.06	0.08
b_1	0.5	0.52	0.55	0.60	0.65	0.70

The larger the value of b_1, the more asymmetry there is in the bar, hence the more the right strut is loaded than the left. The equilibrium program was run for several values of "a" between each of those listed in Table 1 above. The equilibrium program solves for values of p_1, q_1, m_1, and m_2. Values of p_2 and q_2 can then be obtained by Equations 2.63 and 2.64, respectively. Figures 2.10 – 2.14 show how the values of p_1, q_1, m_1, m_2, and the rotation of the bar Φ change as the value of b_1 increases from 0.5 to 0.7. Values of b_1 above 0.7 were not calculated because the rotation is significant at this point, and it would be unrealistic to have a system with a significant amount of rotation in its equilibrium state.

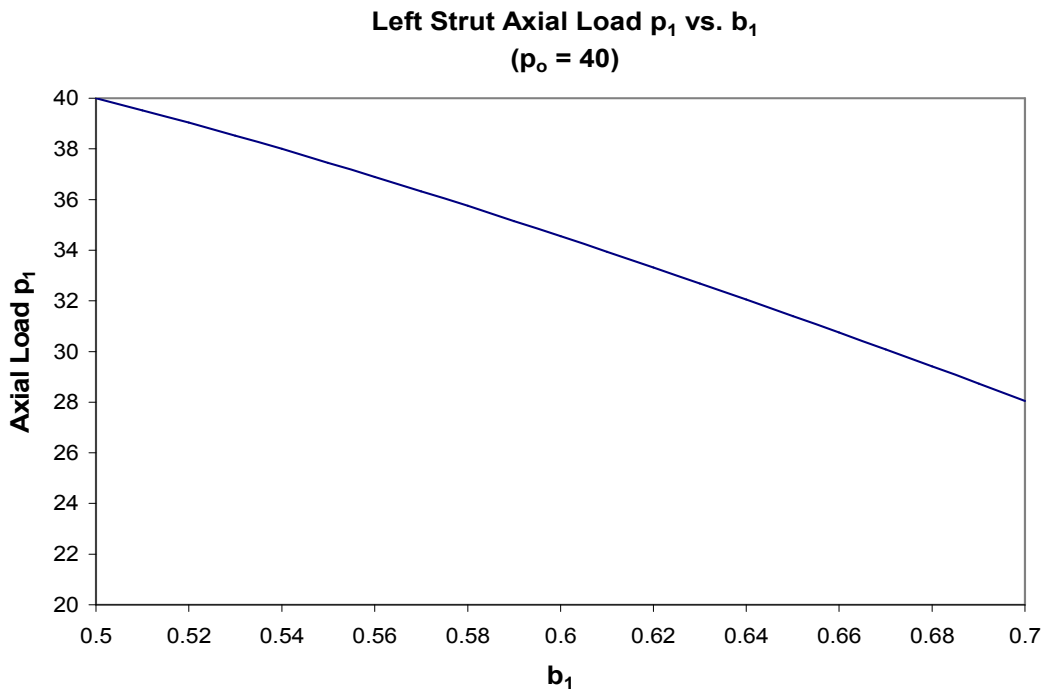

Figure 2.10 Left Strut Axial Load p_1 vs. b_1

As expected, the axial load on the left column decreases as the value of b_1 increases, because the center of mass of the rigid bar is moving away from the left strut. If the axial load of the right strut, p_2, were plotted, it would show the mirror image about $p_1 = 40$ because the sum of p_1 and p_2 is $2p_o$. Because the stiffness of each strut remains the same, the Euler buckling load for each column is still equal to 40. Therefore, the left strut is below the buckling load in all of these cases, and the post-buckled stiffness characteristics required for the system to behave as a vibration isolator are only present in the right strut. Results of this system's performance will be discussed later in the chapter.

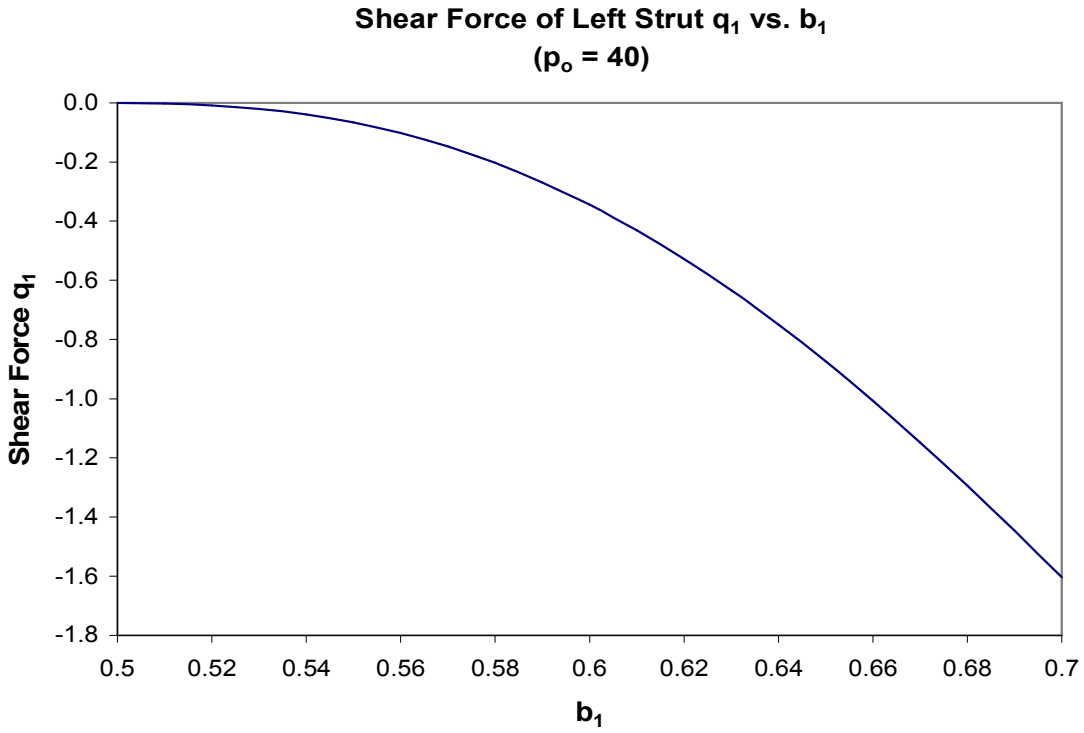

Figure 2.11 Shear Force of Left Strut q_1 vs. b_1

By observing Figure 2.11, we can see that the magnitude of shear force begins to increase dramatically as the value of b_1 increases. Only the left strut shear force is plotted because the right strut shear force is equal and opposite in value. The negative sign only gives the force its direction; the shear force magnitude increases in both struts as the bar becomes more asymmetric. This would be the case for a shift in the center of mass to the left as well as to the right of the center of the bar.

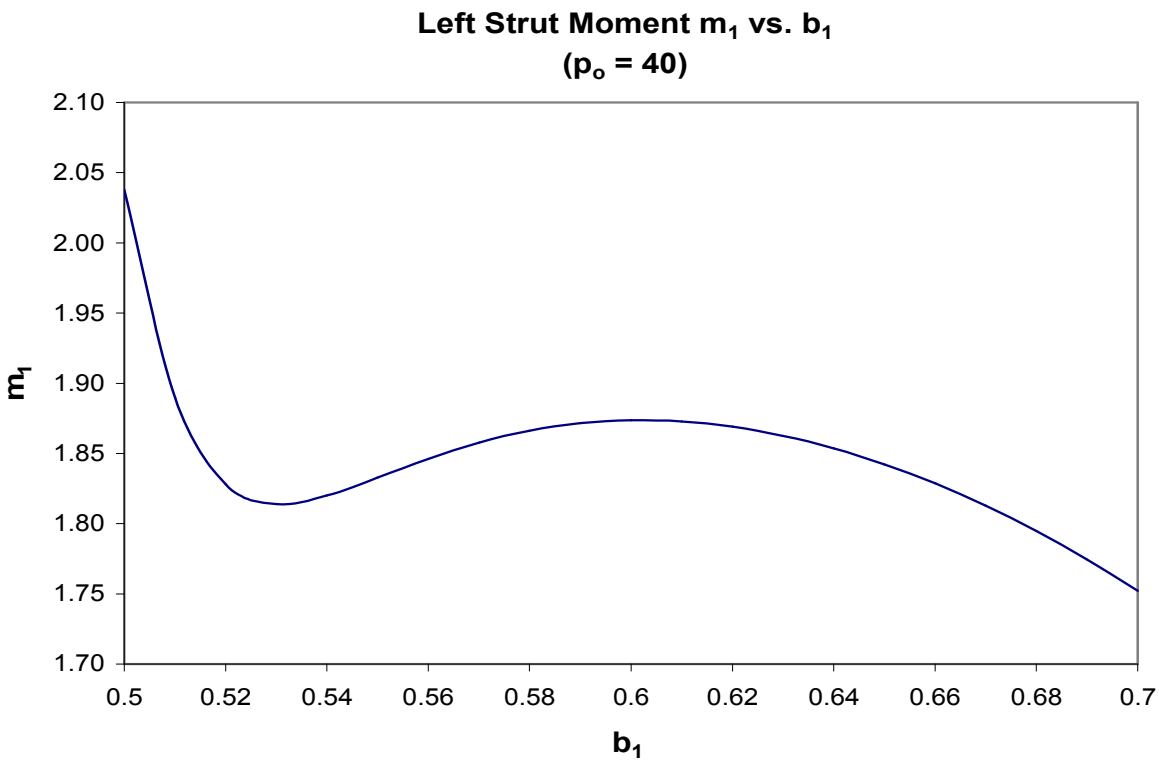

Figure 2.12 Left Strut Moment m_1 vs. b_1

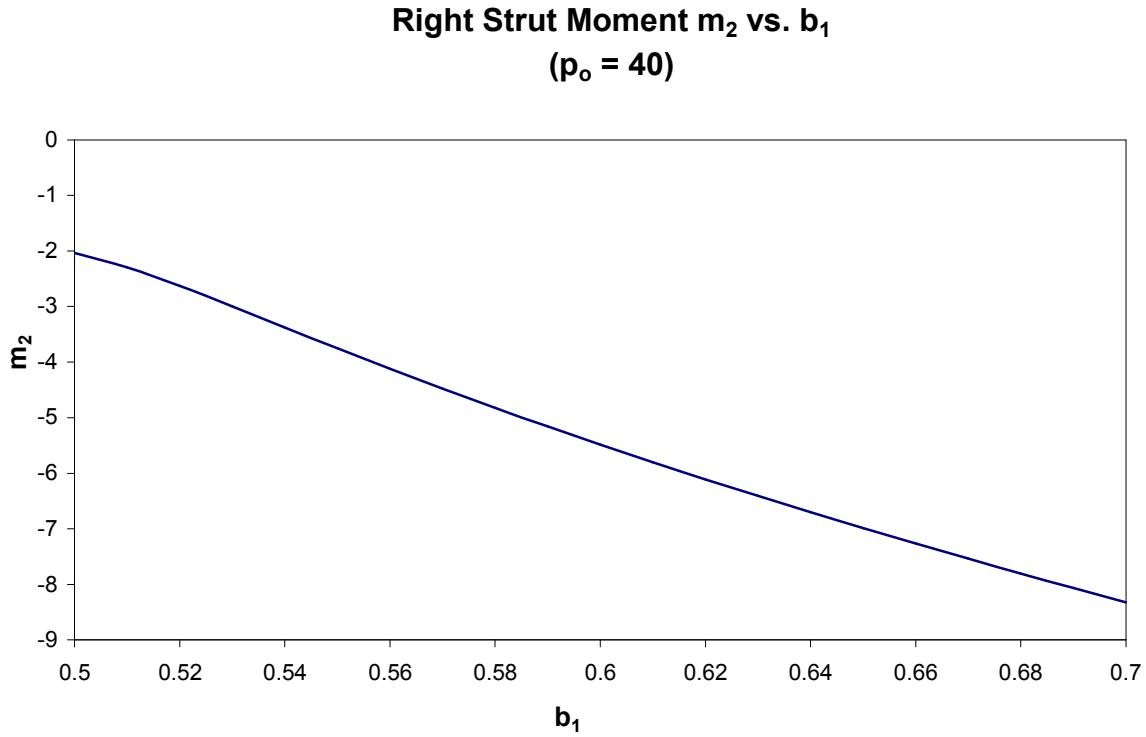

Figure 2.13 Right Strut Moment m_2 vs. b_1

For the symmetric case, the moment in each strut is equal and opposite, and the magnitude is approximately 2.04 when a value of initial load of 40 is used. For the asymmetric case, the moments are not equal and opposite, nor do they vary with the value of b_1 in a similar way. Looking at Figure 2.12, the left strut moment decreases sharply for a slight offset of symmetry, and then increases slightly and levels out at a value of approximately 1.85 until the center of mass has shifted a significant distance to the right of center. However, the right strut moment, shown in Figure 2.13 with a different scale on the ordinate, continues to steadily increase in magnitude (note that the values for the moment are negative) as the center of mass moves closer to the right strut. This is an interesting observation, considering that the axial load in each strut steadily increases or decreases.

The final plot developed is Figure 2.14, which shows how the angle of rotation (in radians) of the bar changes with the shift in center of mass. As expected, the rotation steadily increases. This can also be seen in the deflected shape of the system at equilibrium for different values of b_1 in Figure 2.15.

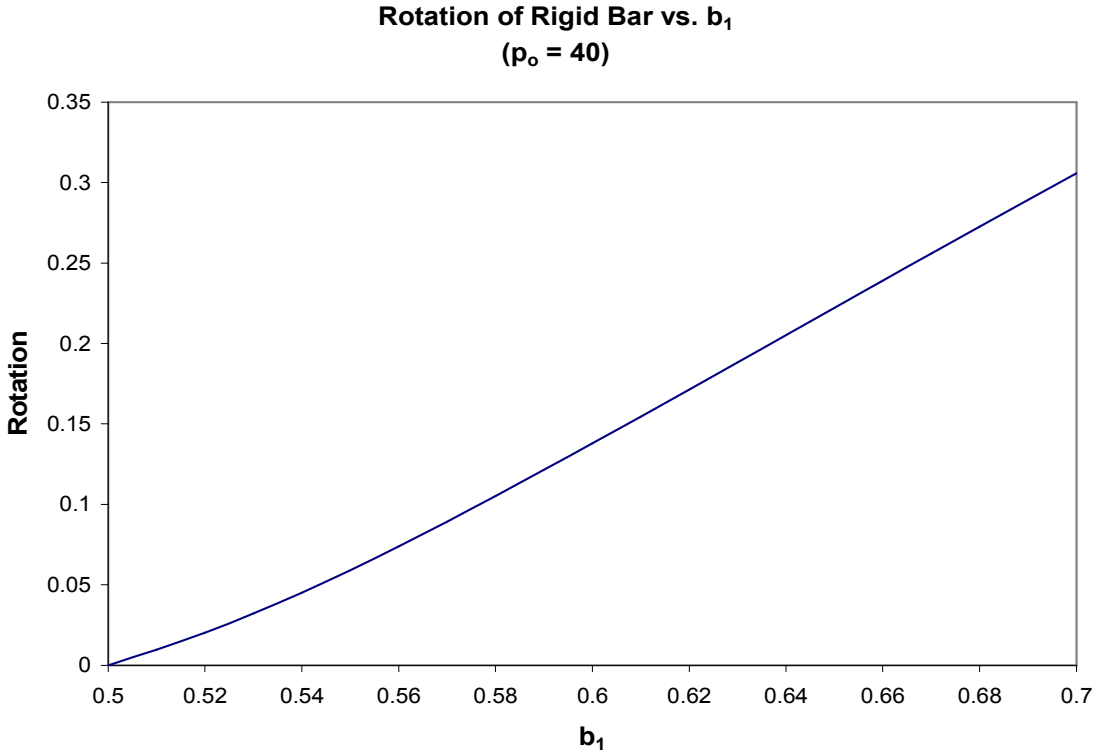

Figure 2.14 Rotation of Rigid Bar vs. b_1

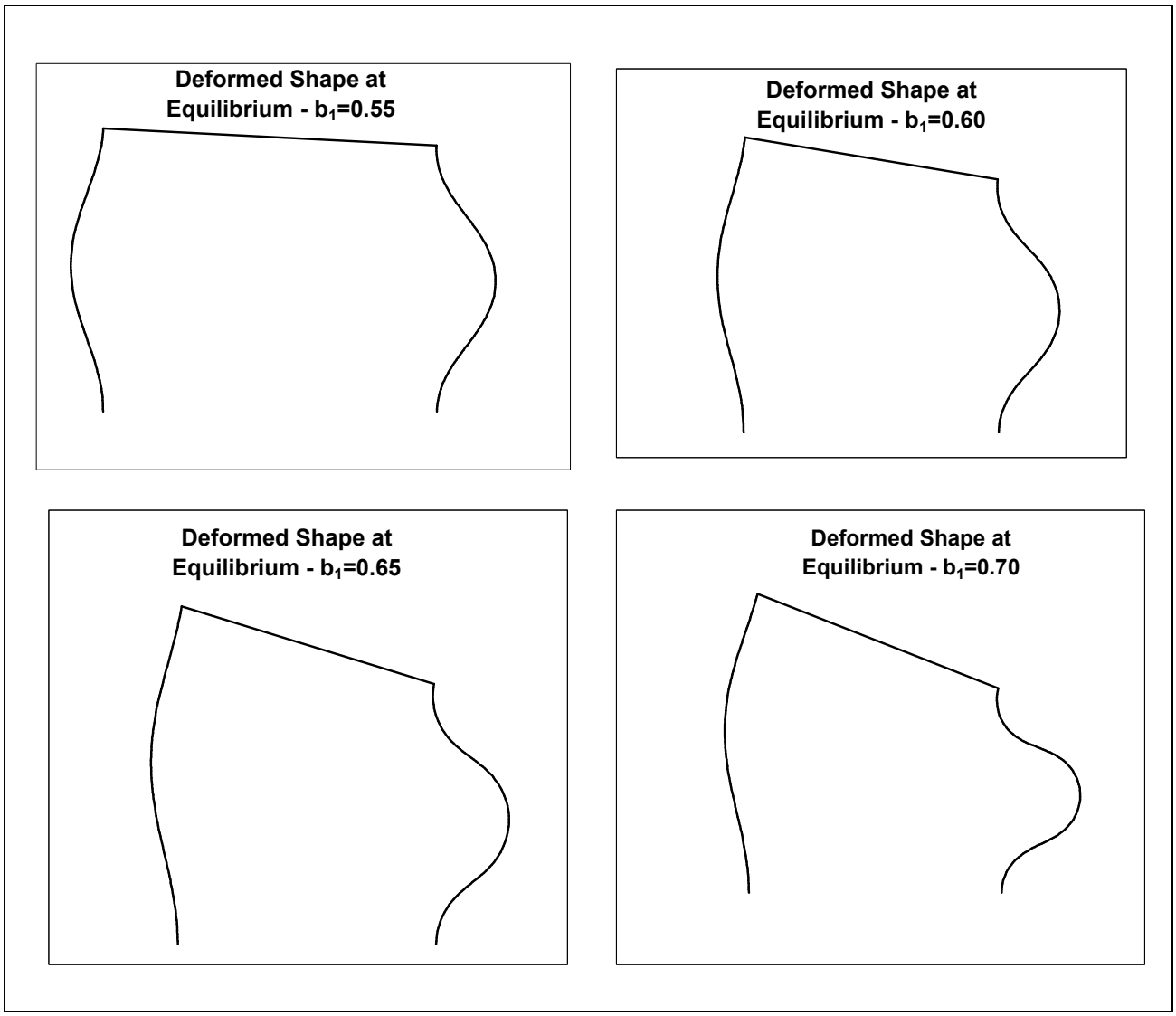

Figure 2.15 Deformed Shape of Model for Different Values of b_1

2.4.3 Dynamic Analysis Procedure

2.4.3.1 Strut Equations

The same equations (Equations 2.35 – 2.40) used to describe the response of the single strut due to a forced harmonic excitation (written as a function of time and location along the strut) are applicable in the asymmetric case as well, except that each strut must have its own set of independent equations. These equations, in nondimensional terms, are written as follows:

$$x_1(s_1,t) = x_{1e}(s_1) + x_{1d}(s_1)e^{i\omega t} \qquad x_2(s_2,t) = x_{2e}(s_2) + x_{2d}(s_2)e^{i\omega t} \qquad (2.77,2.78)$$

$$y_1(s_1,t) = y_{1e}(s_1) + y_{1d}(s_1)e^{i\omega t} \qquad y_2(s_2,t) = y_{2e}(s_2) + y_{2d}(s_2)e^{i\omega t} \qquad (2.79, 2.80)$$

$$\theta_1(s_1,t) = \theta_{1e}(s_1) + \theta_{1d}(s_1)e^{i\omega t} \qquad \theta_2(s_2,t) = \theta_{2e}(s_2) + \theta_{2d}(s_2)e^{i\omega t} \qquad (2.81, 2.82)$$

$$m_1(s_1,t) = m_{1e}(s_1) + m_{1d}(s_1)e^{i\omega t} \qquad m_2(s_2,t) = m_{2e}(s_2) + m_{2d}(s_2)e^{i\omega t} \qquad (2.83, 2.84)$$

$$p_1(s_1,t) = p_{1o} + p_{1d}(s_1)e^{i\omega t} \qquad p_2(s_2,t) = p_{2o} + p_{2d}(s_2)e^{i\omega t} \qquad (2.85, 2.86)$$

$$q_1(s_1,t) = q_{1e} + q_{1d}(s_1)e^{i\omega t} \qquad q_2(s_2,t) = q_{2e} + q_{2d}(s_2)e^{i\omega t} \qquad (2.87, 2.88)$$

Therefore, Equations 2.41-2.46 can also be used, one set for each strut:

$$\frac{dx_{1d}}{ds_1} = -\theta_{1d}\sin\theta_{1e} \qquad \frac{dx_{2d}}{ds_2} = -\theta_{2d}\sin\theta_{2e} \qquad (2.89, 2.90)$$

$$\frac{dy_{1d}}{ds_1} = \theta_{1d}\cos\theta_{1e} \qquad \frac{dy_{2d}}{ds_2} = \theta_{2d}\cos\theta_{2e} \qquad (2.91, 2.92)$$

$$\frac{d\theta_{1d}}{ds_1} = m_{1d} \qquad \frac{d\theta_{2d}}{ds_2} = m_{2d} \qquad (2.93, 2.94)$$

$$\frac{dm_{1d}}{ds_1} = (q_{1d} - p_{1o}\theta_{1d})\cos\theta_{1e} - (p_{1d} + q_{1e}\theta_{1d})\sin\theta_{1e} \qquad (2.95,2.96)$$

$$\frac{dm_{2d}}{ds_2} = (q_{2d} - p_{2o}\theta_{2d})\cos\theta_{2e} - (p_{2d} + q_{2e}\theta_{2d})\sin\theta_{2e} \qquad (2.97,2.98)$$

$$\frac{dp_{1d}}{ds_1} = (\omega^2 - i\omega c)x_{1d} \qquad \frac{dp_{2d}}{ds_2} = (\omega^2 - i\omega c)x_{2d} \qquad (2.99,2.100)$$

$$\frac{dq_{1d}}{ds_1} = (\omega^2 - i\omega c)y_{1d} \qquad \frac{dq_{2d}}{ds_2} = (\omega^2 - i\omega c)y_{2d} \qquad (2.101,2.102)$$

2.4.3.2 Rigid Body Equations

Applying D'Alembert's Principle again, a free body diagram of the inertial forces on the rigid bar is drawn in Figure 2.16, along with the static forces. Note that now the variables

associated with the bar are all functions of time, and the variables along each strut are functions of position on the strut and time.

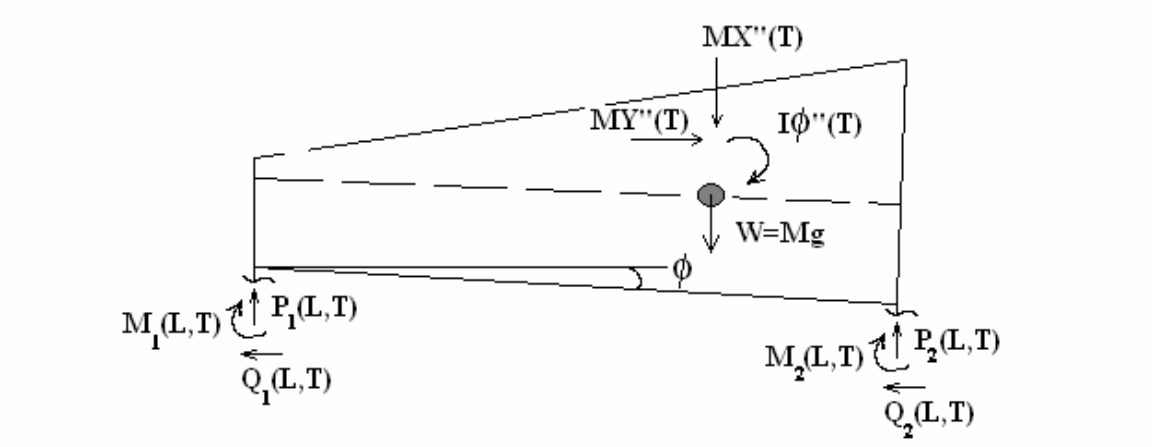

Figure 2.16 Free Body Diagram of Rigid Bar Under Forced Harmonic Vibrations

The following relationships are developed from the free body diagram shown in Figure 2.16

$$M\frac{d^2X(T)}{dT^2} = P_1(L,T) + P_2(L,T) - W \tag{2.103}$$

$$M\frac{d^2Y(T)}{dT^2} = Q_1(L,T) + Q_2(L,T) \tag{2.104}$$

$$\begin{aligned} I_o\frac{d^2\phi(T)}{dT^2} &= P_2(L,T)[B_2\cos\phi(T) + H\sin\phi(T)] - P_1(L,T)[B_1\cos\phi(T) - H\sin\phi(T)] \\ &\quad + Q_2(L,T)[B_2\sin\phi(T) - H\cos\phi(T)] - Q_1(L,T)[B_1\sin\phi(T) + H\cos\phi(T)] \\ &\quad - M_1(L,T) - M_2(L,T) \end{aligned} \tag{2.105}$$

$$\begin{aligned} L + H + X(T) &= X_1(L,T) + H\cos\phi(T) + B_1\sin\phi(T) \\ &= X_2(L,T) + H\cos\phi(T) - B_2\sin\phi(T) \end{aligned} \tag{2.106}$$

$$\begin{aligned} B_2 + Y(T) &= Y_2(L,T) + H\sin\phi(T) + B_2\cos\phi(T) \\ &= B_1 + B_2 + Y_1(L,T) + H\sin\phi(T) - B_1\cos\phi(T) \end{aligned} \tag{2.107}$$

From Equations 2.106 and 2.107,

$$\sin\phi(T) = \frac{[X_2(L,T) - X_1(L,T)]}{B_1 + B_2} \tag{2.108}$$

$$\cos\phi(T) = \frac{[B_1 + B_2 + Y_1(L,T) - Y_2(L,T)]}{B_1 + B_2} \tag{2.109}$$

By substituting Equations 2.108 and 2.109 into Equation 2.105 and evaluating at X=L, we obtain

$$I_o \frac{d^2\phi(T)}{dT^2} =$$
$$\frac{[P_2(L,T)B_2 - P_1(L,T)B_1 - Q_2(L,T)H - Q_1(L,T)H][B_1 + B_2 + Y_1(L,T) - Y_2(L,T)]}{(B_1 + B_2)}$$
$$+ \frac{[Q_2(L,T)B_2 - Q_1(L,T)B_1 + P_2(L,T)H + P_1(L,T)H][X_2(L,T) - X_1(L,T)]}{(B_1 + B_2)}$$
$$- M_1(L,T) - M_2(L,T) \tag{2.110}$$

The final nondimensional quantity to be defined is for the moment of inertia of the bar, I_o, which is defined as

$$i_o = \frac{I_o}{\mu L^3} = \frac{2rp_o}{3h^2}[h^4 + h^2(\frac{b_1 + b_2}{2})^2 + \frac{h^2a^2}{2} - \frac{a^4}{48} - \frac{a^2}{12}(\frac{b_1 + b_2}{2})^2 \tag{2.111}$$

This nondimensional quantity, along with the other nondimensional quantities presented in Equations 2.16-2.22 and 2.48 – 2.64, can be used to rewrite Equations 2.103, 2.104, and 2.106 – 2.109 in nondimensional terms:

$$\frac{d^2x(t)}{dt^2} = \frac{[p_1(1,t) + p_2(1,t) - 2p_0]}{2rp_0} \tag{2.112}$$

$$\frac{d^2y(t)}{dt^2} = \frac{[q_1(1,t) + q_2(1,t)]}{2rp_o} \tag{2.113}$$

$$1 + h + x(t) = x_1(1,t) + h\cos\phi(t) + b_1\sin\phi(t) \tag{2.114}$$
$$= x_2(1,t) + h\cos\phi(t) - b_2\sin\phi(t)$$

$$b_2 + y(t) = y_2(1,t) + h\sin\phi(t) + b_2\cos\phi(t) \qquad (2.115)$$
$$= b_1 + b_2 + y_1(1,t) + h\sin\phi(t) - b_1\cos\phi(t)$$

$$\sin\phi(t) = \frac{[x_2(1,t) - x_1(1,t)]}{b_1 + b_2} \qquad (2.116)$$

$$\cos\phi(t) = \frac{[b_1 + b_2 + y_1(1,t) - y_2(1,t)]}{b_1 + b_2} \qquad (2.117)$$

$$i_o \frac{d^2\phi(t)}{dt^2} = \frac{[p_2(1,t)b_2 - p_1(1,t)b_1 - q_2(1,t)h - q_1(1,t)h][b_1 + b_2 + y_1(1,t) - y_2(1,t)]}{(b_1 + b_2)}$$
$$+ \frac{[q_2(1,t)b_2 - q_1(1,t)b_1 + p_2(1,t)h + p_1(1,t)h][x_2(1,t) - x_1(1,t)]}{(b_1 + b_2)}$$
$$- m_1(1,t) - m_2(1,t) \qquad (2.118)$$

2.4.3.3 Boundary Conditions

To develop expressions for the boundary conditions at $s_1 = s_2 = 1$; the strut and rigid body equations listed above are manipulated as follows:

If Equations 2.116 and 2.117 are substituted into Equation 2.114, the following expression results (for $s_1 = 1$):

$$x(t) = \frac{[b_2 x_1(1,t) + b_1 x_2(1,t) + h y_1(1,t) - h y_2(1,t)]}{b_1 + b_2} - 1 \qquad (2.119)$$

The second derivative is then

$$\frac{d^2x(t)}{dt^2} = \frac{1}{(b_1 + b_2)}[b_2 \frac{\partial^2 x_1(1,t)}{\partial t^2} + b_1 \frac{\partial^2 x_2(1,t)}{\partial t^2} + h\frac{\partial^2 y_1(1,t)}{\partial t^2} - h\frac{\partial^2 y_2(1,t)}{\partial t^2}] \qquad (2.120)$$

When Equation 2.120 above is set equal to Equation 2.112, (because both are expressions for the second derivative of x(t)), the second derivatives with respect to time t of

Equations 2.77 – 2.80 and 2.85, 2.86 are substituted appropriately (hence eliminating the equilibrium portion), and the $[e^{i\omega t}]^2$ term is cancelled from both sides (since we are conducting a linear dynamic analysis), the following expression results:

$$-2\omega^2 rp_o[b_2 x_{1d}(1) + b_1 x_{2d}(1) + hy_{1d}(1) - hy_{2d}(1) = (b_1 + b_2)[p_{1d}(1) + p_{2d}(1)] \tag{2.121}$$

The same manipulation is done for the y component and the Φ component, resulting in the following equations:

$$-2\omega^2 rp_o[b_2 y_{1d}(1) + b_1 y_{2d}(1) + hx_{2d}(1) - hx_{1d}(1) = (b_1 + b_2)[q_{1d}(1) + q_{2d}(1)] \tag{2.122}$$

$$\begin{aligned}\frac{i_o\omega^2[x_{1d}(1) - x_{2d}(1)]}{[b_1 + b_2 + y_{1e}(1) - y_{2e}(1)]} &= p_{2d}(1)b_2 - p_{1d}(1)b_1 - q_{2d}(1)h - q_{1d}(1)h \\ &+ \frac{[y_{1e}(1) - y_{2e}(1)][p_{2d}(1)b_2 - p_{1d}(1)b_1 - q_{2d}(1)h - q_{1d}(1)h]}{(b_1 + b_2)} \\ &+ \frac{[y_{1d}(1) - y_{2d}(1)][p_{2e}(1)b_2 - p_{1e}(1)b_1 - q_{2e}(1)h - q_{1e}(1)h]}{(b_1 + b_2)} \\ &+ \frac{[p_{1d}(1)h + p_{21d}(1)h + q_{2d}(1)b_2 - q_{1d}(1)b_1][x_{2e}(1) - x_{1e}(1)]}{(b_1 + b_2)} \\ &+ \frac{[2p_o h + q_{2e}(1)b_2 - q_{1e}(1)b_1][x_{2d}(1) - x_{1d}(1)]}{(b_1 + b_2)} - m_{1d}(1) - m_{2d}(1)\end{aligned} \tag{2.123}$$

Using trigonometric identities to manipulate Equations 2.116 and 2.117, and substituting the equilibrium relations for $\sin\Phi_e$ and $\cos\Phi_e$, evaluating at $s_1 = s_2 = 1$ gives the boundary condition

$$[x_{2d}(1) - x_{1d}(1)]\sin\phi_e = [y_{2d}(1) - y_{1d}(1)]\cos\phi_e \tag{2.124}$$

As mentioned previously, because the struts are rigidly attached to the bar, and the bar is also assumed to be rigid, it can be assumed that the angle of rotation of the bar, Φ, is

equal to the angles of rotation at the tops of the struts, θ_1 and θ_2. Therefore, the final two boundary conditions needed to solve the system of differential equations are

$$\theta_{1d}(1) = \frac{[x_{2d}(1) - x_{1d}(1)]}{b_1 + b_2} \qquad \theta_{1d}(1) = \theta_{2d}(1) \qquad (2.125, 2.126)$$

Again, a Mathematica program is used to solve the set of differential equations for the range of nondimensional frequencies $0.1<\omega<200$. A text printout of the program is given in Appendix D. Values are set for p_o, a, h, b, c, and r. The values of p_{1e}, p_{2e}, q_{1e}, q_{2e}, $m_{1e,}$ and m_{2e} for the given p_o from the equilibrium analysis are also input values for the program. Initial guesses are given for the values of p_{1d}, p_{2d}, q_{1d}, q_{2d}, m_{1d}, and m_{2d} at $s_1 = 0$ or $s_2 = 0$, and the program solves for these values and for the transmissibility for a given ω. The transmissibility for the system is calculated as an average of the transmissibilities at the top of each strut, which is the transmissibility at the center of the rigid bar. This average transmissibility is the value used in all of the transmissibility versus nondimensional frequency plots presented in the results. The equation for the transmissibility of each strut is the same as for the single strut (Equation 2.47):

$$TR_1 = \frac{\sqrt{\{\mathrm{Re}[x_{1d}(1)]\}^2 + \{I_m[x_{1d}(1)]\}^2}}{|u_o|} \qquad (2.127)$$

$$TR_2 = \frac{\sqrt{\{\mathrm{Re}[x_{2d}(1)]\}^2 + \{I_m[x_{2d}(1)]\}^2}}{|u_o|} \qquad (2.128)$$

$$TR_{avg} = \frac{TR_1 + TR_2}{2} \qquad (2.129)$$